

Journal of Visualized Experiments

Sit-to-stand-and-walk from 120% knee height: A novel approach to assess dynamic postural control. --Manuscript Draft--

Manuscript Number:	JoVE54323R3
Full Title:	Sit-to-stand-and-walk from 120% knee height: A novel approach to assess dynamic postural control.
Article Type:	Invited Methods Article - JoVE Produced Video
Keywords:	Sit-to-stand-and-walk; gait initiation; centre of mass; centre of pressure; motion analysis; physical therapy; rehabilitation
Manuscript Classifications:	14.2.421.784: Rehabilitation; 3.10.228.662: Movement Disorders; 5.1.370.600: Physical Examination; 5.2.831: Rehabilitation; 7.11.427.590.530: Movement; 7.11.427.590.530.389: Gait; 8.2.10.625: Physical Therapy Specialty
Corresponding Author:	Gareth Jones, Ph.D. London South Bank University London, England UNITED KINGDOM
Corresponding Author Secondary Information:	
Corresponding Author E-Mail:	jamesd6@lsbu.ac.uk;Gareth.Jones@gstt.nhs.uk
Corresponding Author's Institution:	London South Bank University
Corresponding Author's Secondary Institution:	
First Author:	Gareth D Jones
First Author Secondary Information:	
Other Authors:	Gareth D Jones Michael Thacker David A Green
Order of Authors Secondary Information:	
Abstract:	<p>Individuals with sensorimotor pathology e.g. stroke have difficulty executing the common task of rising from sitting and initiating gait (sit-to-walk: STW). Thus, in clinical rehabilitation separation of sit-to-stand and gait initiation - termed sit-to-stand-and-walk (STSW) - is usual. However, a standardized STSW protocol with a clearly defined analytical approach suitable for pathological assessment has yet to be defined.</p> <p>Hence, a goal-orientated protocol is defined that is suitable for healthy and compromised individuals by requiring the rising phase to be initiated from 120% knee height with a wide base of support independent of lead limb. Optical capture of three-dimensional (3D) segmental movement trajectories, and force platforms to yield two-dimensional (2D) center-of-pressure (COP) trajectories permits tracking of the horizontal distance between COP and whole-body-center-of-mass (BCOM), the decrease of which increases positional stability but is proposed to represent poor dynamic postural control.</p> <p>BCOM-COP distance is expressed with and without normalization to subjects' leg length. Whilst COP-BCOM distances vary through STSW, normalized data at the key movement events of seat-off and initial toe-off (TO1) during steps 1 and 2 have low intra and inter subject variability in 5 repeated trials performed by 10 young healthy individuals. Thus, comparing COP-BCOM distance at key events during performance of an STSW paradigm between patients with upper motor neuron injury, or other compromised patient groups, and normative data in young healthy individuals is a novel methodology for evaluation of dynamic postural stability.</p>

Powered by Editorial Manager® and ProduXion Manager® from Aries Systems Corporation

5 **TITLE:**

6 Sit-to-stand-and-walk from 120% knee height: A novel approach to assess dynamic postural
7 control independent of lead-limb.

8

9 **AUTHORS:**

10 Jones, Gareth D.

11 Centre for Human and Aerospace Physiological Sciences (CHAPS)

12 Faculty of Life Sciences and Medicine

13 King's College London

14 London, UK

15 and

16 Physiotherapy Department

17 Guy's & St Thomas' NHS Foundation Trust

18 London, UK

19 gareth.jones@gstt.nhs.uk

20

21 James, Darren C.

22 School of Applied Sciences

23 London South Bank University

24 London, UK

25 jamesd6@lsbu.ac.uk

26

27 Thacker, Michael

28 Centre for Human and Aerospace Physiological Sciences (CHAPS)

29 Faculty of Life Sciences and Medicine

30 King's College London

31 London, UK

32 and

33 Physiotherapy Department

34 Guy's & St Thomas' NHS Foundation Trust

35 London, UK

36 michael.thacker@kcl.ac.uk

37

38 Green, David A.

39 Centre for Human and Aerospace Physiological Sciences (CHAPS)

40 Faculty of Life Sciences and Medicine

41 King's College London

42 London, UK

43 david.a.green@kcl.ac.uk

44

45 **CORRESPONDING AUTHOR:**

46 Jones, Gareth D.

47

48 **KEYWORDS:**

49 Sit-to-stand-and-walk, gait initiation, center of mass, center of pressure, motion analysis,
50 physical therapy, rehabilitation

51

52 **SHORT ABSTRACT:**

53 Here, we present a novel protocol to measure positional stability at key events during the
54 sit-to-stand-to-walk using the center-of-pressure to the whole-body-center-of-mass
55 distance. This was derived from the force platform and three-dimensional motion-capture
56 technology. The paradigm is reliable and can be utilized for the assessment of neurologically
57 compromised individuals.

58
59 **LONG ABSTRACT:**

60 Individuals with sensorimotor pathology e.g. stroke have difficulty executing the common
61 task of rising from sitting and initiating gait (sit-to-walk: STW). Thus, in clinical rehabilitation
62 separation of sit-to-stand and gait initiation – termed sit-to-stand-and-walk (STSW) – is
63 usual. However, a standardized STSW protocol with a clearly defined analytical approach
64 suitable for pathological assessment has yet to be defined.

65
66 Hence, a goal-orientated protocol is defined that is suitable for healthy and compromised
67 individuals by requiring the rising phase to be initiated from 120% knee height with a wide
68 base of support independent of lead limb. Optical capture of three-dimensional (3D)
69 segmental movement trajectories, and force platforms to yield two-dimensional (2D)
70 center-of-pressure (COP) trajectories permit tracking of the horizontal distance between
71 COP and whole-body-center-of-mass (BCOM), the decrease of which increases positional
72 stability but is proposed to represent poor dynamic postural control.

73
74 BCOM-COP distance is expressed with and without normalization to subjects' leg length.
75 Whilst COP-BCOM distances vary through STSW, normalized data at the key movement
76 events of seat-off and initial toe-off (TO1) during steps 1 and 2 have low intra and inter
77 subject variability in 5 repeated trials performed by 10 young healthy individuals. Thus,
78 comparing COP-BCOM distance at key events during performance of an STSW paradigm
79 between patients with upper motor neuron injury, or other compromised patient groups,
80 and normative data in young healthy individuals is a novel methodology for evaluation of
81 dynamic postural stability.

82
83 **INTRODUCTION:**

84 Clinical pathologies affecting the sensorimotor systems, for example upper motor neuron
85 (UMN) injury following stroke, lead to functional impairments including weakness, loss of
86 postural stability and spasticity, which can negatively affect locomotion. Recovery can be
87 variable with a significant number of stroke survivors failing to achieve the functional
88 milestones of safe standing or walking^{1,2}.

89
90 The discrete practice of walking and sit-to-stand are common rehabilitative tasks after UMN
91 pathology^{3,4}, however transitional movements are frequently neglected. Sit-to-walk (STW) is
92 a sequential postural-locomotor task incorporating sit-to-stand (STS), gait initiation (GI), and
93 walking⁵.

94
95 Separation of STS and GI, reflective of hesitation during STW has been observed in patients
96 with Parkinson's disease⁶ and chronic stroke⁷, in addition to older unimpaired adults⁸, but
97 not in young healthy individuals⁹. Therefore sit-to-stand-and-walk (STSW) is commonly
98 implemented within the clinical environment and is defined by a pause phase of variable

99 length when standing. However, there are no published protocols to date defining STSW
100 dynamics in a context suitable for patient populations.

101

102 Usually in STW studies the initial chair height is 100% of knee height (KH; floor-to-knee
103 distance), foot-width and GI lead-limb are self-selected, arms are constrained across the
104 chest and an ecologically meaningful task context is often absent⁵⁻⁹. However, patients find
105 rising from 100% KH challenging¹⁰ and frequently adopt a wider foot position compared
106 with healthy individuals¹¹, initiate gait with their affected leg⁷, and use their arms to
107 generate momentum⁷.

108

109 To initiate gait, a state change in whole-body movement in a purposeful direction is
110 required¹². This is achieved by uncoupling the whole-body center-of-mass (BCOM: the
111 weighted average of all considered body segments in space¹³) from the center-of-pressure
112 (COP: the position of the resultant ground reaction force (GRF) vector¹⁴). In the anticipatory
113 phase of GI, rapid stereotypical posterior and lateral movement of the COP toward the limb
114 to be swung occurs thereby generating BCOM momentum^{12,15}. The COP and BCOM are thus
115 separated, with the horizontal distance between them having been proposed as a measure
116 of dynamic postural control¹⁶.

117

118 The calculation of COP-BCOM distance requires simultaneous measurement of the COP and
119 BCOM positions. The standard calculation of COP is shown below in equation (1)¹⁷:

120

121

$$COP_x = \frac{((Origin_z * Force_x) - M_y)}{Force_z}$$

122

$$COP_y = \frac{(M_x + (Origin_z * Force_y))}{Force_z}$$

123

$$COP_z = Origin_z$$

124 (1)

125

126 Where M and Force represent moments about the force platform axes and the directional
127 GRF respectively. The subscripts represent axes. The origin is the vertical distance between
128 the contact surface and the origin of the force platform, and is considered to be zero.

129

130 The kinematic method of deriving BCOM position involves tracking the displacement of
131 segmental markers. A faithful representation of body-segment motion can be achieved by
132 employing markers clustered on rigid plates placed away from bony landmarks, minimizing
133 soft-tissue-artifact (CAST technique¹⁸). In order to determine BCOM position, individual
134 body segment masses are estimated, based on cadaveric work¹⁹. Three-dimensional (3D)
135 motion system proprietary software uses the coordinate positions of proximal and distal
136 segment locations to: 1) determine segmental lengths, 2) arithmetically estimate segmental
137 masses, and 3) compute segmental COM locations. These models are then able to provide
138 estimates of 3D BCOM position at a given point in time based on the net summation of
139 inter-segmental positions (Figure 1).

140

141 [Place Figure 1 here]

142

143 Thus, the purpose of this paper is first to present a standardized STSW protocol that is
144 ecologically valid and includes rising from a high seat-height. It has been shown previously
145 that STSW from 120% KH is biomechanically indistinct from 100% KH barring generation of
146 lower BCOM vertical velocities and GRF's during rising²⁰, meaning rising from 120% KH is
147 easier (and safer) for compromised individuals. Second, to derive COP-BCOM horizontal
148 distances to assess dynamic postural control during key milestones and transitions using 3D
149 motion-capture. This approach, which in healthy individuals during STSW is independent of
150 limb-lead²⁰, offers the prospect of functional recovery evaluation. Finally, a preliminary
151 STSW data set representative of young healthy individuals is presented, and intra and inter-
152 subject variability in the group is defined in order to inform comparison with pathological
153 individuals.

154

155 **PROTOCOL:**

156

157 The protocol follows the local guidelines for the testing of human participants, defined by
158 London South Bank University research ethics committee approval (UREC1413/2014).

159

160 **1. Gait Laboratory Preparation**

161

162 1.1 Clear the capture volume of unwanted reflective objects that may be misinterpreted
163 as movement markers and eliminate ambient daylight to reduce reflections as appropriate.

164

165 1.2 Turn on motion-capture cameras, proprietary tracking software, force platform
166 amplifiers, and external analogue-to-digital (AD) converter. Allow time for the cameras to
167 initialize.

168

169 1.3 Arrange cameras ensuring that there are at least 2 intersecting axes at the extremes
170 of the capture volume. Ensure individual cameras have optimal exposure and aperture
171 settings by checking individual point-resolution of test markers (e.g. the static calibration
172 frame) within capture volume space (see Reference Appendix A²¹).

173

174 1.4 Mount subject-switch to turn off visual go signal in the midline of the walkway, 6 m
175 in front of the starting position in the direction of travel, on a tripod at subject's navel
176 height. Mount light source (for visual go signal) in the midline of the walkway, 1 m in front
177 of the subject-switch in the direction of travel, on a tripod at subject's canthus height
178 (Figure 2). Arrange the operator light switch in close proximity to the investigator.

179

180 1.5 Arrange force platforms 1 and 2 in parallel for gait-initiation, and force platforms 3
181 and 4 in a staggered configuration to capture non-dominant lead-limb trials. Then attach
182 force platform covers with removable tape.

183

184 [Place Figure 2 here].

185

186 1.6 In the proprietary tracking software set capture frequency to 60 Hz and 3D tracking
187 parameters. Specifically, use a prediction error of 20 mm, a maximum residual of 2 mm,

188 minimum trajectory length equivalent to 2 frames, and a maximum frame gap of 10 frames.
189 Go on to identify each of the 8 individual force platform components (z1, z2, z3, z4, x1-2, X3-
190 4, y1-4, y2-3) from each form platform amplifier into the respective analog to digital
191 converter (32 channels in this study).

192

193 1.6.1 Ensure all pre-determined calibration settings from each force platform's calibration
194 documentation, scaling factors and analogue channels have been specified (see chapter
195 Project Options; Analogue Boards²¹) and nominate offset to be read during the last 10
196 frames of capture when unloaded.

197

198 1.7 In the proprietary tracking software, nominate a multiplier to the motion-capture
199 frequency to ensure an adequate analogue sampling frequency. Use a multiplier of 17,
200 yielding an individual force platform sampling frequency of 1020 Hz.

201

202 1.8 Implement the dynamic wand calibration procedure:

203

204 1.8.1 Place the L-shaped reference structure in the measurement volume with the long
205 axis pointing in the anterior direction (see chapter Wand calibration method²¹).

206

207 1.8.2 In the **Calibration settings** page in the **Project options** dialog, select the calibration
208 'type' to Wand, with a 750 mm length. Then select coordinate system orientation with
209 positive z-axis pointing upwards and positive y-axis as the long arm (see chapter
210 Calibration²¹). Click **OK**.

211

212 1.8.3 Click the **Calibration icon** and set the intended length of the calibration capture to 60
213 sec. Then set a time delay of 5 sec and identify the file directory where the results will be
214 saved. Click **OK** to commence calibrating.

215

216 Note: The wand procedure uses two calibration objects to calibrate the measurement
217 volume; this is used to maximize the resolution of a large motion capture volume (Figure 3).
218 One is a stationary L-shaped reference structure with four markers attached to it and is used
219 to define the global coordinate system. The other object is a wand, which consists of two
220 markers located a fixed distance from each other. During calibration, the x, y, z orientations
221 of these are tracked with respect to the x, y, z positions of the four static markers on the
222 reference structure; in turn permitting the proprietary software to triangulate, predict and
223 reconstruct the trajectories of the moving markers in 3D space. At the end of this process,
224 each camera will return a residual error of its accuracy.

225

226 [Place Figure 3 here].

227

228 1.8.4 Move the calibration wand in the measurement volume and proceed to rotate the
229 wand around the intended capture volume for the specified 60 sec (see chapter Wand
230 Calibration Method²¹).

231

232 1.8.5 Check the **Calibration results**, accept calibration with individual camera residual
233 errors of <1.5 mm, click **OK**.

234

235 Note: If you have force plates there will be a warning reminding you of measuring the force
236 plate position again (since it has most probably changed with the new calibration).

237

238 1.9 Remove calibration set from capture volume. Locate the force platforms in the
239 calibrated 3D space by placing one 12 mm diameter passive retro-reflective marker in each
240 of the 4 corners of each platform (attention to placement is essential; see chapter Force
241 Plate Location²¹). Obtain a 5 sec recording and proceed to identify each marker and each
242 platform's reference system (PRS) within the 3D space as per proprietary software
243 suggestions.

244

245 1.10 Undertake a dynamic capture using the aforementioned sampling and 3D tracking
246 parameters (1.6) to confirm and sense-check subsequent force magnitudes and directions.

247

248 1.10.1 Set up dynamic capture for 60 sec with a 10 sec delay. Once the click to **commence**
249 **capture** is initiated, the operator has time to sit on the stool, pause, stand, pause and walk
250 forwards making contact with the force platforms (at this point, there is no need for the
251 operator to have retro-reflective markers attached in situ).

252

253 1.10.2 Once the capture has finished, check the direction and magnitudes of ground
254 reaction vectors to ensure configurations of force-platforms are correct. Expect upward and
255 posterior to direction of travel vectors at foot contact, and a maximum vertical force of
256 approximately 1 to 1.5 times body weight.

257

258 1.11 Place height adjustable stool in the midline of the capture volume between force
259 platforms 1 and 2 (Figure 2), then connect a 300 mm diameter pressure seat-mat to the
260 external AD converter.

261

262 1.12 Prepare all passive retro-reflective anatomical markers for fixation by pre attaching
263 individually to one side of double adhesive tape, approximately 15 mm in length (at least 60
264 cm of double adhesive tape in total per subject) and arrange in an appropriate location
265 ready for application to subject. Include tracking marker clusters and self-securing bandage
266 ready for timely subject application.

267

268 Note: Tracking markers should comprise a minimum of 3 retro-reflective markers arranged
269 in a non-co-linear arrangement, and are placed on body segments (some anatomical
270 markers positioned at estimated joint centers can be used as tracking markers e.g. 1st and
271 5th metatarsals).

272

273 2. **Subject Preparation**

274

275 2.1 Obtain written informed consent from subject who fulfills inclusion/exclusion
276 criteria.

277

278 2.2 Ask subject to change into suitable clothing (cycling shorts, close fitting t-shirt and
279 sports bra as appropriate).

280

281 2.3 Establish dominant lower limb using the kicking-a-ball test²² if the subject is able to

282 safely do so.

283

284 2.4 Measure subject standing height (m) and mass (kg); convert mass to weight (N).

285

286 2.5 With subject standing, measure subject bi-acromial distance (m) using measuring
287 calipers. Lock caliper position to use distance for feet positioning (see 4.5 below).

288

289 2.6 Measure vertical floor-to-knee distance (m) on the dominant limb (in standing);
290 multiply distance by 1.2 to calculate 120% KH distance (m). Adjust stool height to 120% KH.
291 Table 1 summarizes 10 healthy subject characteristics including knee height data.

292

293 [Place Table 1 here]

294

295 2.7 Prepare the skin areas for marker placement. Shave unwanted body hair as
296 appropriate and use alcohol wipes to remove excess sweat and/or moisturizer to maximize
297 adherence between markers and the skin.

298

299 2.8 Palpate, identify and apply retro-reflective markers to anatomical landmarks of the
300 lower and upper extremities, trunk, head and pelvic segments in accordance with the
301 chosen technical frame of reference²³ (Table 2). Go on to apply segmental tracking markers
302 with self-securing bandage.

303

304 Note: In females, if difficulty arises locating the sternal notch marker - place marker over the
305 center of the sports bra garment.

306

307 [Place Table 2 here]

308

309 2.9 Ask subject to walk into the capture volume and adopt the anatomical position.

310

311 Note: At this point the subject must not move until after static capture has been performed
312 due to the inherent problem of estimating the hip joint center over clothing at this
313 anatomical location.

314

315 3. **Static Capture**

316

317 3.1 Instruct subject to stand stationary in the center of the calibrated volume, assuming
318 the standard anatomical position, with all anatomical and tracking markers in situ.

319

320 Note: In order to reduce soft tissue artifact a static calibration is undertaken with
321 anatomical and tracking markers in situ. The tracking markers are referenced to the
322 anatomical markers, which negates the limitation of assuming that joint centers do not
323 move under the skin. Tracking markers are left in situ for subsequent dynamic trials. This is
324 termed the calibrated anatomical systems technique (CAST)¹⁸.

325

326 3.1.1 In order to undertake a short static capture, use the aforementioned sampling and
327 3D tracking parameters (1.6) and ensure all markers are accounted for in the capture
328 volume by confirming the total number of markers listed in the **Unidentified Trajectories**

329 panel in 3D real-time mode. This should correspond with the total number of markers that
330 the chosen technical frame of reference requires. Click the **record icon** to complete a 5 sec
331 capture. Repeat procedure where necessary if markers are missing.

332

333 Note: See section 6 below for the processing of static capture data.

334

335 3.2 Use the position data from the hip-joint-center landmark on the subject dominant
336 side to determine leg-length (distance from hip-joint-center (see 7.1 and Table 3b below) to
337 floor) for distance normalization (see 7.12 below).

338

339 **4. Familiarization**

340

341 4.1 Remove all anatomical-only markers.

342

343 4.2 Instruct subject to sit on the stool with feet on individual force platforms 1 & 2.

344

345 4.3 Instruct subject to stand and then walk forward with the defined leading leg. Adjust
346 the anteroposterior position of the stool until the subject consistently makes central contact
347 with force platforms 3 and 4 during the first 2 steps of gait. Allow repeated practice trials
348 until the subject is comfortable.

349

350 4.4 Mark the front leg position of the stool with tape on the floor surface in order to re-
351 establish stool position.

352

353 4.5 Set up final feet position (Figure 2). Ask subject to sit on the stool with feet on
354 individual force platforms 1 and 2. Adjust shank position on subject's dominant side 10°
355 posterior from vertical using an extendable arm goniometer. Go on to adjust the non-
356 dominant foot equally in line, and then using the locked calipers (see 2.5 above), arrange
357 the inter-foot width to the pre-determined bi-acromial distance accordingly between the
358 lateral foot borders.

359

360 4.6 Adjust the transverse plane orientation of each foot such that each medial foot
361 border is placed in line with the direction of travel.

362

363 4.7 After finally checking alignment, draw around final foot positions using a dry board
364 marker pen onto the removable force platform surface.

365

366 4.8 Use the verbal instruction: "When you see the light come on in front of you, stand up
367 and stop. Mentally count down from 3 to 1, one number at a time. Then, leading with your
368 non-dominant leg, walk at a comfortable pace toward the switch in front of the light and
369 stop. Count mentally from 3 down to 1, one number at a time, and then with your writing
370 hand use the switch to turn off the light".

371

372 4.9 Re-iterate to the subject that they may use their arms naturally, then allow the
373 subject sufficient familiarization to STSW protocol. Familiarization gives the subject as much
374 time as possible to acclimatize to the testing environment ensuring they are able to
375 efficiently accomplish the task without any forced movement that might otherwise impinge

376 on the ecological validity of the experimental paradigm.

377

378 **5. STSW Dynamic Trials**

379

380 5.1 With subject sitting on the stool ready for dynamic trials, first confirm the total
381 number of markers listed in the **Unidentified Trajectories** panel in 3D real-time mode and
382 that they correspond with the total number of markers that the chosen technical frame of
383 reference requires. Then click the **record icon** to complete a 60 sec dynamic capture.

384

385 5.2 After 5 sec capture, turn on the operator light-switch and check how the subject
386 responds - that they rise from the stool and pause as instructed, step on to force platforms
387 3 and 4, and that they stop and turn the light off as instructed within the capture period.

388

389 5.3 Re-set the light switch and check for marker dropouts by accounting for all markers
390 during slow motion playback of trial. Repeat if necessary, otherwise continue to next trial.
391 Go on to capture 5 trials of STSW in each subject.

392

393 5.4 In the event of anatomical markers becoming unattached, re-attach to
394 predetermined skin mark. If tracking markers move, re-attach anatomical markers and a
395 repeat static trial – then continue with remaining dynamic trials.

396

397 **6. Proprietary Tracking Software Post Processing**

398

399 6.1 In proprietary tracking software, identify and label all markers from static and
400 dynamic trials (see chapter Manual Identification of Trajectories²¹) and crop unwanted
401 capture by moving the time-slides to the beginning and end of the task. Utilize the
402 “automatic identification of markers”, otherwise known as **AIM**, functionality in the
403 proprietary tracking software to aid labeling (see chapter Generating an AIM Model²¹).

404

405 Note: Labeling of markers is required so that the proprietary and subsequent biomechanics
406 analysis software consistently constructs and calculates the relative trajectory of a rigid
407 body in 3-dimensional space. Use meaningful labeling as shown in Table 2. **AIM** is subject-
408 specific, but continually updates. With a different subject and in the event of a poor AIM, go
409 on to update **AIM** by manual labelling. This also applies to the static capture process (see
410 section 3.2 above).

411

412 6.2 In the event of marker drop out, that exceeds 10 frames, go on to either locate the
413 missing trajectory in the **Unidentified Trajectories** panel, or manually **gap-fill** using the
414 polynomial interpolation function provided by the proprietary software (see chapter Gap Fill
415 Trajectories²¹).

416

417 Note: In some cases marker trajectories are partially absent and gap-filling is a mechanism
418 whereby missing data can be mathematically estimated based on the measured trajectory
419 before and after the missing data.

420

421 6.3 Format and export all static and dynamic trials, in **c3d** format, for post-processing in
422 biomechanics analysis software.

423

424 Note: Prior to export, exclude all unidentified and empty marker trajectories, specifying de
425 facto labeling, and nominate the last 10 frames for zero force baseline levels for each force
426 plate.

427

428 **7. Biomechanics Analysis Software Post Processing**

429

430 7.1 Build static 13-segment model²³ (feet, shanks, thighs, pelvis, trunk, upper arms,
431 forearms and head (note no hands).

432

433 Note: The process of model building is fundamental in defining the linked segments based
434 on the static measurement trial and proprietary software instructions were used²⁴. In this
435 protocol the anatomical coordinate systems for each body segment (Table 3a) and joint
436 center locations (Table 3b) are based mainly on Ren *et al.*²³ with adaptations to avoid
437 functional hip and glenohumeral joint center estimation. Gold standards for all joint center
438 locations remain imaging techniques such as magnetic resonance imaging (MRI), which are
439 unrealistic in most situations. Functional joint center estimations have been utilized;
440 however, there remains the risk that patients with pathology would not be able to move the
441 joint in the requisite planes²⁵. Therefore, for the pelvis regression equations e.g. Davis²⁶ are
442 often used. Here, the CODA pelvis²⁷ was used and is based on work by Bell *et al.*²⁸, and the
443 glenohumeral joint centers were estimated according to Eames *et al.*²⁹.

444

445 [Place Table 3a and Table 3b here]

446

447 7.2 Import the dynamic files and assign the model to each. Confirm accuracy of model
448 building by checking normal visual configuration of segments. In the case of inaccuracy, the
449 operator is advised to go back to the proprietary tracking software files and check sensor
450 image tracking profiles and correct as necessary.

451

452 7.3 Low pass filter kinematic and kinetic data using a 4th order Butterworth filter with
453 cut-off frequency at 6 Hz and 25 Hz respectively.

454

455 7.4 Average filter light and pressure-mat analogue signals over a 25-frame window.

456

457 7.5 Create force structure for force platforms 1, 2, 3, and 4. Use corner coordinates to
458 create a level-surfaced, rectangular structure encompassing all 4 force platforms (Figure 4).

459

460 Note: A force structure is required³⁰ in order that net COP calculations can be made across
461 the 4 force platforms.

462

463 7.6 Calculate the net COP coordinate signals (x and y) within the laboratory coordinate
464 system (LCS) from the force structure.

465

466 Note: The software performs this by using equations 2a-g below:

467

468 [Place Figure 4 here]

469

470 (2a) Net medio-lateral force

$$F_x = \sum_{i=1}^4 F_{xi}$$

471 (2b) Net anterior-posterior force

$$F_y = \sum_{i=1}^4 F_{yi}$$

472 (2c) Net vertical force

$$F_z = \sum_{i=1}^4 F_{zi}$$

473 (2d) Net platform moment about x-axis

$$M_x = \sum_{i=1}^4 (Y_i + y_i) * F_{zi}$$

474 (2e) Net platform moment about y-axis

$$M_y = \sum_{i=1}^4 -(X_i + x_i) * F_{zi}$$

475 (2f) x-Coordinate of net force application point (COP_x)

$$COP_x = \frac{-M_y}{F_z}$$

476 (2g) y-Coordinate of net force application point (COP_y)

$$COP_y = \frac{M_x}{F_z}$$

477 7.6.1 Use x and y signals from equations 2f and 2g for net COP position within the LCS.

478

479 7.7 Using customized pipeline commands, create important movement events within
480 STSW, specifically seat-off, upright, gait initiation onset, first toe-off 1, and 1st and 2nd initial
481 contacts (Table 4).

482

483 [Place Table 4 here]

484

485 7.8 Using customized pipeline commands calculate the COP-BCOM distance (L) by
486 applying equation 3 at each movement event, where t_i represents a given event.

487

$$L(t_i) = \sqrt{[(x_{COP}(t_i)) - (x_{BCOM}(t_i))]^2 + (y_{COP}(t_i)) - (y_{BCOM}(t_i))]^2}$$

488 (3)

489

490 7.9 Using customized pipeline commands, calculate the maximum COP-BCOM distance
491 (L_{max}) by applying equation 4 between two events ($t_o \rightarrow t_i$).

492

493

$$L_{max} = \max_{0 \leq t \leq i} \left\{ \sqrt{[(x_{COP}(t_i)) - (x_{BCOM}(t_i))]^2 + (y_{COP}(t_i)) - (y_{BCOM}(t_i))]^2} \right\}$$

494 (4)

495

496 where: t_o and t_i represent movement onset and the final time instance of interest
497 respectively, $(x_{COP}(t_i))$ is the x coordinate of the COP at time t_i , $(x_{BCOM}(t_i))$ is the x
498 coordinate of the BCOM at time t_i , and $(y_{COP}(t_i))$ and $(y_{BCOM}(t_i))$ are the corresponding
499 values for the y coordinates³¹.

500

501 7.10 Extract dependent variables of interest at movement events; COP-BCOM distances
502 at seat-off and first toe-off (TO1) events, and maximum COP-BCOM distances during the 1st

496 step phase (between TO1 and first initial-contact; IC1) and the 2nd step phase (between IC1
497 and IC2) using customized pipeline commands.

498

499 7.11 Normalize intra-subject COP-BCOM distances as a proportion of subject's dominant
500 leg length (see 3.3 above).

501

502 7.12 Export data for statistical analysis using the **Copy to Clipboard** functionality or by
503 exporting files in other available native formats.

504

505 **8. Lab-specific normative value calculations.**

506

507 8.1 Calculate mean (± 1 SD) intra and inter-subject values for both actual COP-BCOM
508 distances and normalized values as proportions of subjects' dominant lower limb length.

509

510 8.2 Calculate coefficients of variation (COV) for mean inter-subject data.

511

512 8.3 Calculate intra-subject variation per event using two-way mixed effects model intra-
513 class correlation coefficients ($ICC_{3,1}$), and the measurement error³².

514

515 **REPRESENTATIVE RESULTS:**

516 All subjects rose with their feet placed on the twin force platforms, leading with their non-
517 dominant limb as instructed. Normal gait was observed with subjects stepping cleanly onto
518 the other platforms and 3D optical-based motion analysis successfully tracked whole body
519 movement during 5 repeated goal-orientated STSW tasks rising from 120% KH.

520 Simultaneous COP and BCOM mediolateral (ML) and anteroposterior (AP) displacements
521 between seat-off and IC2 (100% STSW cycle) comprising: rise, pause, gait initiation (GI), step
522 1, and step 2 are shown respectively in Figure 4A and 4B for the first subject (left leg (non-
523 dominant) lead). In the ML plane, there was negligible COP or BCOM displacement from
524 seat-off to GI onset. However, after GI onset COP displaces leftward away from the standing
525 limb toward the swing limb – separating from the BCOM, which displaces rightward. Then,
526 the COP laterally displaces rightward toward the subsequent stance limb, passing beyond
527 the BCOM rightward before toe-off. Thereafter, during steps 1 and 2, the BCOM follows a
528 sinusoidal displacement, with the COP displacing further laterally during single limb stance
529 (Figure 5A).

530

531 [Place Figure 5 here]

532

533 In the AP plane, the COP at seat-off starts in front of the BCOM, and while they both move
534 forward during rising; their separation diminishes steadily before merging at upright. After
535 the pause phase the BCOM accelerates forwards through GI and steps 1 and 2. In contrast,
536 the COP displaces backwards at GI onset and then forward after toe-off but remains behind
537 the BCOM throughout step 1. The COP, however, passes in front of the BCOM during step 2
538 after initial contact 1 likely to correspond with the transition to single limb stance. COP
539 forward displacement then slows and passes behind the BCOM again just before mid-
540 stance/swing (Figure 5B).

541

542 The horizontal separation distance between COP and BCOM, throughout the STSW cycle,

543 provides a composite of the planar description of COP and BCOM displacements. This
544 approach simplifies the complex interaction of COP and BCOM displacement providing an
545 index of positional stability (Figure 5C).

546

547 Intra-subject COP-BCOM separation distances were consistent at seat-off, TO1, and during
548 step 1 and 2 by virtue of strong intraclass correlation coefficients at all 4 events. In addition,
549 the measurement error (Table 5), or common standard deviation of repeated measures³²,
550 was small: 9 mm (seat-off) and 12 mm (TO1, step 1, step 2) across all subjects. Another
551 useful way to present measurement error is the repeatability statistic (Table 5). It
552 represents the magnitude of the expected difference between 2 repeated measures 95% of
553 the time, and is between 24 mm and 34 mm for the 4 events.

554

555 Inter-subject COP-BCOM separation distances were consistent (Table 6) at seat-off and TO1,
556 in addition to during step 1 and 2. In this homogenous, healthy adult group; subject leg-
557 length range (0.803-0.976 m (Table 1))³³ and variance was small (mean 0.855 m; SD 0.051
558 m). Whilst it is not typical to normalize COP-BCOM distances to leg length and Figure 6
559 shows negligible differences between normalized and un-normalized inter-subject mean
560 COP-BCOM data, normalization does reduce the coefficient of variance (COV; Table 6).

561

562 [Place Table 5 here]

563

564 [Place Table 6 here]

565

566 [Place Figure 6 here]

567

568 **Figure 1: 2D BCOM calculation.** For simplicity, the example is based on calculating whole-leg
569 COM from a 3-linked mass in 2 dimensions, where coordinates of the respective COM
570 positions (x, y), and segmental masses (m_1, m_2, m_3) are known. Segment masses and location
571 of segmental COM positions, with respect to the laboratory coordinate system (LCS; origin:
572 0, 0), are estimated by motion analysis system proprietary software using subject body mass
573 and published anthropometric data (see main text). The x and y leg COM position, in this
574 example of the 3-linked mass, is then derived using the formulae shown.

575

576 **Figure 2: Experimental Protocol.** This example shows a left-leg lead: Subjects sit on an
577 instrumented stool at 120% knee height (KH) with ankles 10° degrees in dorsiflexion and
578 feet at shoulder width apart orientated forward. On a visual cue, subjects perform 5 trials of
579 STSW leading with their non-dominant limb at self-selected pace terminated by switching
580 off the light.

581

582 **Figure 3: L-Shaped Reference Structure and Wand for Camera Calibration.** The L-shaped
583 reference structure remains stationary and has 4 markers attached to it. The wand has two
584 markers attached to it at a fixed distance and is moved, with respect to the reference
585 structure, to create a 3-D calibrated volume of space that is sufficient enough for the
586 intended marker set to pass through.

587

588 **Figure 4: Force Structure.** Example of a rectangular force structure encompassing 4 force
589 platforms in a right lead-limb orientation. Details of local COP application and dimensions

590 with respect to a laboratory coordinate system (LCS) are shown for force platform 1 as an
591 example. The x , y , z position of the platform reference system (PRS) is offset relative to the
592 LCS where X_1 and Y_1 represent the mediolateral and anteroposterior distances from PRS,
593 respectively. To calculate the individual platform moment about the x -axis, the vertical GRF
594 is multiplied by the sum of the local y COP coordinate and the new PRS-LCS offset y
595 coordinate (Y_1+y_1). The moment about the y -axis coordinate is similarly calculated by
596 multiplying the vertical GRF by the negative sum of the local x COP coordinate and the new
597 PRS-LCS offset x coordinate $-(X_1+x_1)$. The total moment of force about the global force
598 structure is equal to the sum of all of the moments of force, divided by the sum of the
599 individual vertical forces. Net COP X and Y coordinates are thus produced for the force
600 structure within the LCS (equations 2a-g).

601
602 **Figure 5: COP and BCOM Displacements.** Panels show the first subject undertaking STSW
603 from 120% KH with non-dominant limb-lead; in this case left-leg lead. The time axis is
604 normalized to percentage time between seat-off and initial contact 2 (IC2). A) Mediolateral
605 displacement. Y -axis direction labels with respect to the swing (left) leg. Lines show COP and
606 BCOM data corresponding to each trial, the bold lines represents the mean, and shaded
607 areas represent $\pm 1SD$ around the mean. B) Anteroposterior displacements. Y -axis direction
608 labels with respect to the swing (left) leg. Lines show COP and BCOM data corresponding to
609 each trial, the bold lines represents the mean, and shaded areas represent ± 1 SD around the
610 mean. C) COP-BCOM horizontal distance. Lines show distance data corresponding to each
611 trial, the bold line represents the mean, and shaded area represents ± 1 SD around the
612 mean. Seat-off and toe-off 1 events, and maxima during steps 1 and 2 are marked.

613
614 **Figure 6: Within and Between-Subject COP-BCOM Distances.** A) Un-Normalized. Each line
615 represents within-subject mean COP-BCOM distance. The bold line represents the between-
616 subject mean distance. B) Normalized to Dominant Leg Length. Each line represents within-
617 subject mean COP-BCOM distance as a percentage of the subject's dominant leg length. The
618 bold line represents the between-subject mean distance as a percentage of the subject's
619 dominant leg length.

620
621 **Table 1: Subject Characteristics.** Individual data and mean (± 1 SD) across 10 subjects are
622 shown

623
624 **Table 2: Marker-set placement.** Markers (anatomical and tracking) based on a previously
625 reported technical frame of reference²³.

626
627 **Table 3a: Anatomical Coordinate System for Whole Body Model.**

628
629 **Table 3b: Joint Center Definitions for Whole Body Model.**

630
631 **Table 4: Movement Event Definitions.**

632
633 **Table 5: COP-BCOM Distances.** Intra (5 trials) and inter-subject mean ± 1 SD data is shown as
634 actual distances and normalized to subject non-dominant leg length for discrete distances at
635 seat-off and TO1, and maximum distances during step 1 and step 2.

636

637 **Table 6: Intra-subject variation.** ICCs (95% confidence interval) and measurement error
638 (mean intra-subject SD distance in m) and repeatability statistics³² are shown per event.

639

640 **DISCUSSION:**

641 The sit-to-stand-and-walk (STSW) protocol defined here can be used to test dynamic
642 postural control during complex transitional movement in healthy individuals or patient
643 groups. The protocol includes constraints that are designed to allow subjects with pathology
644 to participate, and the inclusion of switching off the light means it is ecologically valid and
645 goal-orientated. As it has been shown previously that lead-limb and rising from a high (120%
646 KH) seat does not fundamentally affect task dynamics during STSW²⁰, the methods
647 described here can be applied as a standard protocol. This STSW protocol has validity
648 because compared to healthy individuals, patients find rising from low seat heights a
649 challenge¹⁰, tend to generate less horizontal momentum⁷ and separate rising before
650 initiating gait from a wide foot position¹¹ with their affected leg⁷. This paper also describes
651 how to calculate COP and BCOM displacement during STSW, from which the horizontal
652 separation between COP and BCOM – an index of dynamic stability¹⁶ - can be derived
653 between seat-off and the second step.

654

655 The results are dependent on a number of critical steps within the protocol. Firstly, the
656 removal of artefactual light and optimal camera exposure settings is required to ensure the
657 accuracy of optical 3D marker tracking. Secondly, attention to the capture volume when
658 calibrating is an important consideration to further optimize motion capture accuracy.
659 Thirdly, force plate synchronization with the motion capture system using an appropriate
660 scale factor reduces the potential for error in the magnitude of the resultant ground
661 reaction force vector. Fourthly, precise force plate identification in the 3D space is critical.
662 Special care must be made when locating each plate's PRS, and validation of this accuracy
663 must be a routine³⁴. This ensures that force plate structure and rendering during post-
664 processing is optimized for the presentation of high quality COP data. Finally, the main
665 contributors to BCOM displacement estimation errors are inaccurate marker positioning,
666 locating of joint centers and skin movement artifacts³⁵. Thus, experience in anatomical
667 palpation and adoption of the CAST method¹⁸ should be considered prerequisites. Other
668 techniques involve using fewer markers or even a singular estimator of BCOM position
669 during gait such as sacral inertial sensors. However, this technique requires validation³⁶ and
670 is of limited utility when body segment orientations deviate from those when upright i.e.
671 during rise³⁷. Thus, multiple camera quantification of BCOM remains the gold standard
672 technique for STSW.

673

674 With these steps considered in a healthy population, intra-subject variability during STSW is
675 low, justifying averaging across trials with a high degree of confidence. Furthermore, low
676 (healthy) inter-subject variability suggests comparison with such (lab specific) normative
677 data would provide high sensitivity to differences induced by pathology. Whilst, inter-
678 subject variability was low, reduced COV can be achieved by normalizing for leg length. One
679 aspect that warrants further investigation is the STSW pause phase. Healthy subjects self-
680 selected a mean (\pm SD) pause phase of 0.84 sec (\pm 0.07). Whether this differs in pathological
681 groups, and if so whether there is any effect upon stability during transition remains to be
682 determined.

683

684 The degree of COP-BCOM separation varies during the different phases of STSW. The largest
685 COP-BCOM distances were at seat-off, TO1, and just prior to foot contact during steps 1 and
686 2. These represent the biggest challenge to the postural control systems and are therefore
687 defined as the events of interest. Decreased COP-BCOM separation is associated with
688 increased positional stability, but indicates reduced postural stability³¹. At seat-off as the
689 body transitions from a stable to an unstable base of support, positional stability is
690 accomplished either by posterior positioning of the feet or anterior positioning of the trunk
691 relative to the seat, both of which are commonly seen in functionally impaired patients^{38,39}.
692 After pause, BCOM-COP distances increase during GI; incorporating the anticipatory,
693 postural “release” and “unloading” sub-phases¹⁵, and a locomotor swinging limb phase. The
694 end of GI and start of step 1 occurs at TO1; where a relative increase in COP-BCOM
695 separation is associated with BCOM forward acceleration caused by the combined GI
696 phases, the outcome of which is higher walking velocity⁴⁰. Therefore, COP-BCOM distance at
697 seat-off and TO1 represent candidate dynamic postural stability variables to be tested in
698 pathological groups.

699
700 In addition, maximum COP-BCOM distance peaks occur consistently during steps 1 and 2 at
701 the end of single support. These are important events to measure because steps 1 and 2
702 represent the period where steady-state gait is realized. Larger mean COP-BCOM distances
703 during step 1 compared to step 2 in all but one healthy subject using the protocol were
704 observed. Step 1 remains part of the locomotor acceleration phase before steady-state gait
705 is reached at the end of step 2¹². Therefore, step 1 is subject to both postural and locomotor
706 control demands and is more positionally unstable than subsequent steps in gait; a feature
707 supported by the increased risk of falling during every day transitional movements⁴¹. Step 2
708 is no less important as it represents the commencement of steady-state gait. Therefore,
709 maximum COP-BCOM distances during both steps 1 and 2 phases are indicated in STSW
710 analysis.

711
712 In conclusion, this STSW protocol extends the use of COP-BCOM horizontal separation to
713 STSW and our preliminary results provide an initial normative data set for healthy
714 individuals. COP-BCOM distances normalized to leg length at seat-off, TO1, and step 1 and 2
715 maxima during performance of a goal-orientated STSW paradigm is a novel methodology for
716 evaluation of dynamic postural stability. It offers the possibility of deriving highly consistent
717 normative global or local data sets that can be compared with UMN injured patients or
718 other compromised patient groups.

719

720 **ACKNOWLEDGMENTS**

721 The authors would like to thank Tony Christopher, Lindsey Marjoram at King’s College
722 London and Bill Anderson at London Southbank University for their practical support. Thank
723 you also to Eleanor Jones at King’s College London for her help in collecting the data for this
724 project.

725

726 **DISCLOSURES:**

727 The authors have no competing financial interests to disclose.

728

729 **REFERENCES:**

730 1 Duncan, P. W., Goldstein, L. B., Matchar, D., Divine, G. W. & Feussner, J.

731 Measurement of motor recovery after stroke. Outcome assessment and sample size
732 requirements. *Stroke* **23** (8), 1084-1089, doi:10.1161/01.STR.23.8.1084 (1992).

733 2 Smith, M. T. & Baer, G. D. Achievement of simple mobility milestones after stroke.
734 *Arch Phys Med Rehabil* **80** (4), 442-447, doi: [http://dx.doi.org/10.1016/S0003-](http://dx.doi.org/10.1016/S0003-9993(99)90283-6)
735 9993(99)90283-6 (1999).

736 3 Langhorne, P., Bernhardt, J. & Kwakkel, G. Stroke rehabilitation. *Lancet* **377** (9778),
737 1693-1702, doi:10.1016/S0140-6736(11)60325-5 (2011).

738 4 Veerbeek, J. M. *et al.* What is the evidence for physical therapy poststroke? A
739 systematic review and meta-analysis. *PLoS One* **9** (2), e87987,
740 doi:10.1371/journal.pone.0087987 (2014).

741 5 Magnan, A., McFadyen, B. & St-Vincent, G. Modification of the sit-to-stand task with
742 the addition of gait initiation. *Gait Posture* **4** (3), 232-241, doi:
743 [http://dx.doi.org/10.1016/0966-6362\(95\)01048-3](http://dx.doi.org/10.1016/0966-6362(95)01048-3) (1996).

744 6 Buckley, T. A., Pitsikoulis, C. & Hass, C. J. Dynamic postural stability during sit-to-walk
745 transitions in Parkinson disease patients. *Mov Disord* **23** (9), 1274-1280,
746 doi:10.1002/mds.22079 (2008).

747 7 Frykberg, G. E., Aberg, A. C., Halvorsen, K., Borg, J. & Hirschfeld, H. Temporal
748 coordination of the sit-to-walk task in subjects with stroke and in controls. *Arch Phys Med*
749 *Rehabil* **90** (6), 1009-1017, doi:10.1016/j.apmr.2008.12.023 (2009).

750 8 Dehail, P. *et al.* Kinematic and electromyographic analysis of rising from a chair
751 during a "Sit-to-Walk" task in elderly subjects: role of strength. *Clin Biomech (Bristol, Avon)*
752 **22** (10), 1096-1103, doi:10.1016/j.clinbiomech.2007.07.015 (2007).

753 9 Buckley, T., Pitsikoulis, C., Barthelemy, E. & Hass, C. J. Age impairs sit-to-walk motor
754 performance. *J Biomech* **42** (14), 2318-2322, doi:10.1016/j.jbiomech.2009.06.023 (2009).

755 10 Roy, G. *et al.* The effect of foot position and chair height on the asymmetry of
756 vertical forces during sit-to-stand and stand-to-sit tasks in individuals with hemiparesis. *Clin*
757 *Biomech (Bristol, Avon)* **21** (6), 585-593, doi:10.1016/j.clinbiomech.2006.01.007 (2006).

758 11 Kubinski, S. N., McQueen, C. A., Sittloh, K. A. & Dean, J. C. Walking with wider steps
759 increases stance phase gluteus medius activity. *Gait Posture* **41** (1), 130-135,
760 doi:10.1016/j.gaitpost.2014.09.013 (2015).

761 12 Jian, Y., Winter, D. A., Ishac, M. G. & Gilchrist, L. Trajectory of the body COG and COP
762 during initiation and termination of gait. *Gait Posture* **1** (1), 9-22,
763 doi:[http://dx.doi.org/10.1016/0966-6362\(93\)90038-3](http://dx.doi.org/10.1016/0966-6362(93)90038-3) (1993).

764 13 Winter, D. A. Human balance and posture control during standing and walking. *Gait*
765 *Posture* **3** (4), 193-214, doi:[http://dx.doi.org/10.1016/0966-6362\(96\)82849-9](http://dx.doi.org/10.1016/0966-6362(96)82849-9) (1995).

766 14 Cavanagh, P. R. A technique for averaging center of pressure paths from a force
767 platform. *J Biomech* **11** (10-12), 487-491, doi:[http://dx.doi.org/10.1016/0021-](http://dx.doi.org/10.1016/0021-9290(78)90060-X)
768 9290(78)90060-X (1978).

769 15 Halliday, S. E., Winter, D. A., Frank, J. S., Patla, A. E. & Prince, F. The initiation of gait
770 in young, elderly, and Parkinson's disease subjects. *Gait Posture* **8** (1), 8-14, doi:
771 [http://dx.doi.org/10.1016/S0966-6362\(98\)00020-4](http://dx.doi.org/10.1016/S0966-6362(98)00020-4) (1998).

772 16 Hass, C. J., Waddell, D. E., Fleming, R. P., Juncos, J. L. & Gregor, R. J. Gait initiation
773 and dynamic balance control in Parkinson's disease. *Arch Phys Med Rehabil* **86** (11), 2172-
774 2176, doi:10.1016/j.apmr.2005.05.013 (2005).

775 17 Winter, D. A., Patla, A. E., Ishac, M. & Gage, W. H. Motor mechanisms of balance
776 during quiet standing. *J Electromyogr Kinesiol* **13** (1), 49-56, doi:
777 [http://dx.doi.org/10.1016/S1050-6411\(02\)00085-8](http://dx.doi.org/10.1016/S1050-6411(02)00085-8) (2003).

778 18 Cappozzo, A., Catani, F., Croce, U. D. & Leardini, A. Position and orientation in space
779 of bones during movement: anatomical frame definition and determination. *Clin Biomech*
780 *(Bristol, Avon)* **10** (4), 171-178, doi: [http://dx.doi.org/10.1016/0268-0033\(95\)91394-T](http://dx.doi.org/10.1016/0268-0033(95)91394-T)
781 (1995).

782 19 Dempster, W. T., Gabel, W. C. & Felts, W. J. The anthropometry of the manual work
783 space for the seated subject. *Am J Phys Anthropol* **17** (4), 289-317,
784 doi:10.1002/ajpa.1330170405 (1959).

785 20 Jones, G. D., James, D. C., Thacker, M., Jones, E. J. & Green, D. A. Sit-to-Walk and Sit-
786 to-Stand-and-Walk Task Dynamics are Maintained During Rising at an Elevated Seat-Height
787 Independent of Lead-Limb in Healthy Individuals. *Gait Posture* (under review)

788 21 Qualysis AB. *Qualysis Track Manager User Manual* (Sweden: Author, 2011).

789 22 Hoffman, M., Schrader, J., Applegate, T. & Koceja, D. Unilateral postural control of
790 the functionally dominant and nondominant extremities of healthy subjects. *J Athl Train* **33**
791 (4), 319-322, doi: <http://www.ncbi.nlm.nih.gov/pubmed/16558528> (1998).

792 23 Ren, L., Jones, R. K. & Howard, D. Whole body inverse dynamics over a complete gait
793 cycle based only on measured kinematics. *J Biomech* **41** (12), 2750-2759,
794 doi:10.1016/j.jbiomech.2008.06.001 (2008).

795 24 C-Motion Wiki Documentation. *Tutorial: Building a Model*, <[http://www.c-
796 motion.com/v3dwiki/index.php/Tutorial:_Building_a_Model](http://www.c-motion.com/v3dwiki/index.php/Tutorial:_Building_a_Model)> (2013).

797 25 Kainz, H., Carty, C. P., Modenese, L., Boyd, R. N. & Lloyd, D. G. Estimation of the hip
798 joint centre in human motion analysis: a systematic review. *Clin Biomech (Bristol, Avon)* **30**
799 (4), 319-329, doi:10.1016/j.clinbiomech.2015.02.005 (2015).

800 26 Harrington, M. E., Zavatsky, A. B., Lawson, S. E., Yuan, Z. & Theologis, T. N. Prediction
801 of the hip joint centre in adults, children, and patients with cerebral palsy based on
802 magnetic resonance imaging. *J Biomech* **40** (3), 595-602,
803 doi:10.1016/j.jbiomech.2006.02.003 (2007).

804 27 C-Motion Wiki Documentation. *Coda Pelvis*, <[http://www.c-
805 motion.com/v3dwiki/index.php/Coda_Pelvis](http://www.c-motion.com/v3dwiki/index.php/Coda_Pelvis)> (2015).

806 28 Bell, A. L., Brand, R. A. & Pedersen, D. R. Prediction of hip joint centre location from
807 external landmarks. *Human movement science* **8** (1), 3-16,
808 doi:[http://dx.doi.org/10.1016/0167-9457\(89\)90020-1](http://dx.doi.org/10.1016/0167-9457(89)90020-1) (1989).

809 29 Eames, M. H. A., Cosgrove, A. & Baker, R. Comparing methods of estimating the total
810 body centre of mass in three-dimensions in normal and pathological gaits. *Human*
811 *movement science* **18** (5), 637-646, doi:[http://dx.doi.org/10.1016/S0167-9457\(99\)00022-6](http://dx.doi.org/10.1016/S0167-9457(99)00022-6)
812 (1999).

813 30 C-Motion Wiki Documentation. *Force Structures*, <[http://www.c-
814 motion.com/v3dwiki/index.php?title=Force_Structures](http://www.c-motion.com/v3dwiki/index.php?title=Force_Structures)> (2015).

815 31 Martin, M. *et al.* Gait initiation in community-dwelling adults with Parkinson disease:
816 comparison with older and younger adults without the disease. *Phys Ther* **82** (6), 566-577,
817 doi: <http://ptjournal.apta.org/content/82/6/566.full.pdf> (2002).

818 32 Bland, J. M. & Altman, D. G. Measurement error. *BMJ* **313** (7059), 744, doi:
819 <http://dx.doi.org/10.1136/bmj.313.7059.744> (1996).

820 33 Hof, A. L. Scaling gait data to body size. *Gait Posture* **4** (3), 222-223,
821 doi:10.1016/0966-6362(95)01057-2 (1996).

822 34 Holden, J. P., Selbie, W. S. & Stanhope, S. J. A proposed test to support the clinical
823 movement analysis laboratory accreditation process. *Gait Posture* **17** (3), 205-213, doi:
824 <http://www.ncbi.nlm.nih.gov/pubmed/12770634> (2003).

825 35 Baker, R. Gait analysis methods in rehabilitation. *J Neuroeng Rehabil* **3** 4,
826 doi:10.1186/1743-0003-3-4 (2006).

827 36 Gregory, C. M., Embry, A., Perry, L. & Bowden, M. G. Quantifying human movement
828 across the continuum of care: From lab to clinic to community. *J Neurosci Methods* **231** 18-
829 21, doi:10.1016/j.jneumeth.2014.04.029 (2014).

830 37 Pai, Y. C. & Rogers, M. W. Segmental contributions to total body momentum in sit-
831 to-stand. *Medicine and Science in Sports and Exercise* **23** (2), 225-230, doi:
832 <http://europepmc.org/abstract/MED/2017019> (1991).

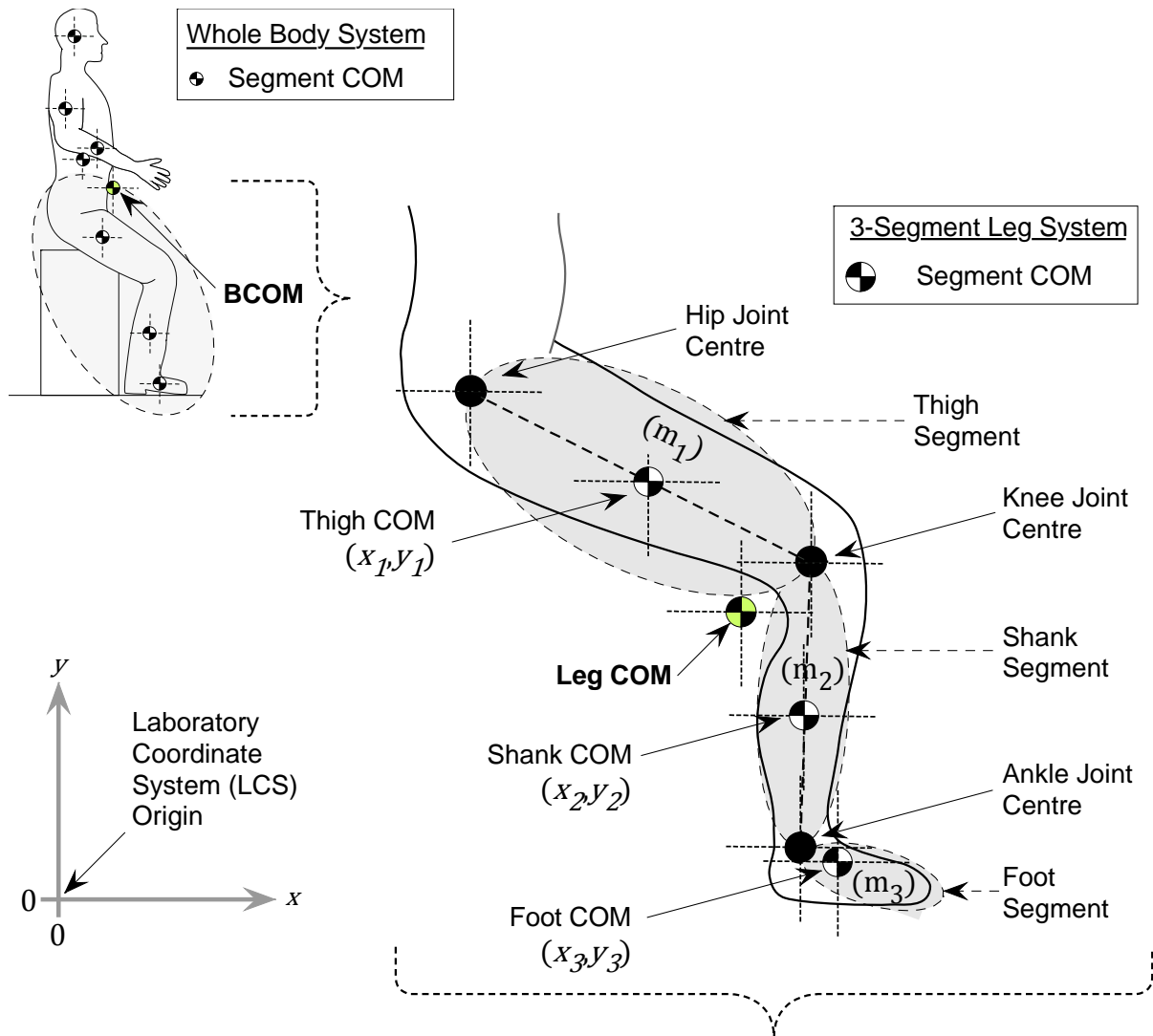
833 38 Hughes, M. A., Weiner, D. K., Schenkman, M. L., Long, R. M. & Studenski, S. A. Chair
834 rise strategies in the elderly. *Clin Biomech (Bristol, Avon)* **9** (3), 187-192, doi:
835 [http://dx.doi.org/10.1016/0268-0033\(94\)90020-5](http://dx.doi.org/10.1016/0268-0033(94)90020-5) (1994).

836 39. Medeiros DL de, Conceição JS, Graciosa MD, Koch DB, Santos MJ Dos, Ries LGK. The
837 influence of seat heights and foot placement positions on postural control in children with
838 cerebral palsy during a sit-to-stand task. *Res Dev Disabil* **43-44**, 1–10,
839 doi:10.1016/j.ridd.2015.05.004 (2015).

840 40 Breniere, Y. & Do, M. C. When and how does steady state gait movement induced
841 from upright posture begin? *J Biomech* **19** (12), 1035-1040, doi:
842 [http://dx.doi.org/10.1016/0021-9290\(86\)90120-X](http://dx.doi.org/10.1016/0021-9290(86)90120-X) (1986).

843 41 Weerdesteyn, V., de Niet, M., van Duijnhoven, H. J. & Geurts, A. C. Falls in individuals
844 with stroke. *J Rehabil Res Dev* **45** (8), 1195-1213, doi:10.1682/JRRD.2007.09.0145 (2008).

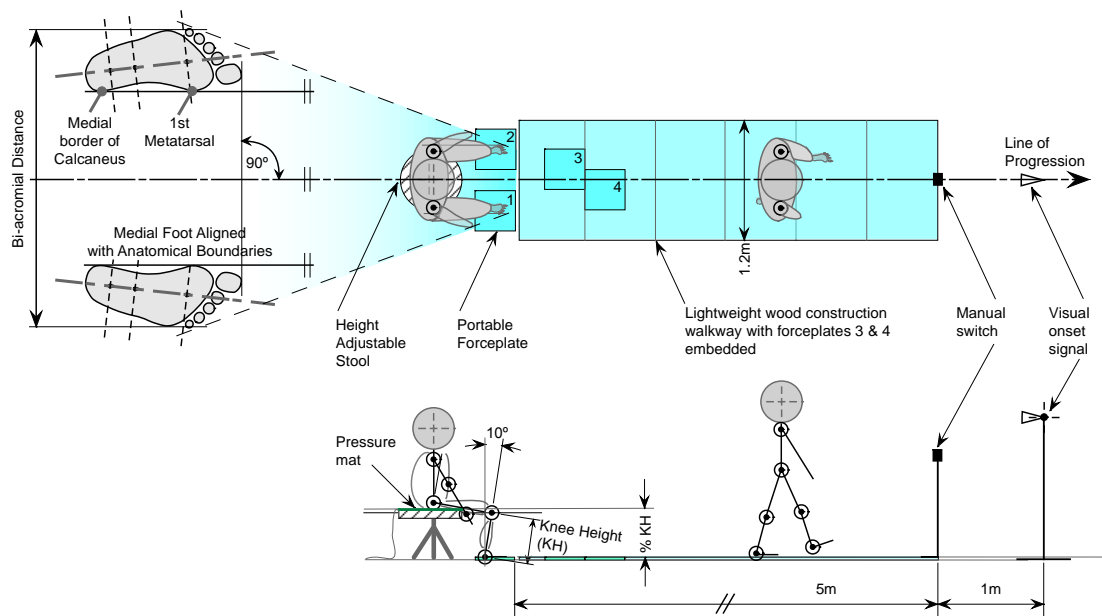
845
846
847
848
849
850
851
852
853
854
855
856
857
858
859
860
861
862
863
864
865
866
867
868
869
870



$$LegCOM_x = \frac{x_1.m_1 + x_2.m_2 + x_3.m_3}{m_1 + m_2 + m_3}$$

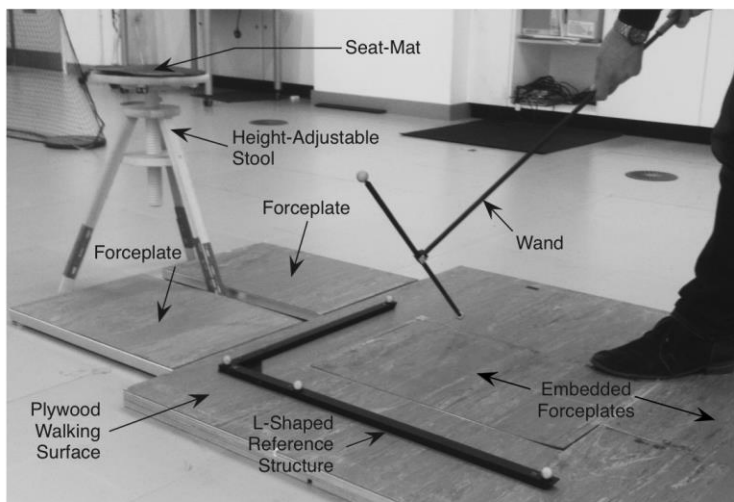
$$LegCOM_y = \frac{y_1.m_1 + y_2.m_2 + y_3.m_3}{m_1 + m_2 + m_3}$$

871
 872 Figure 1.
 873
 874
 875
 876
 877
 878
 879
 880
 881
 882
 883
 884
 885



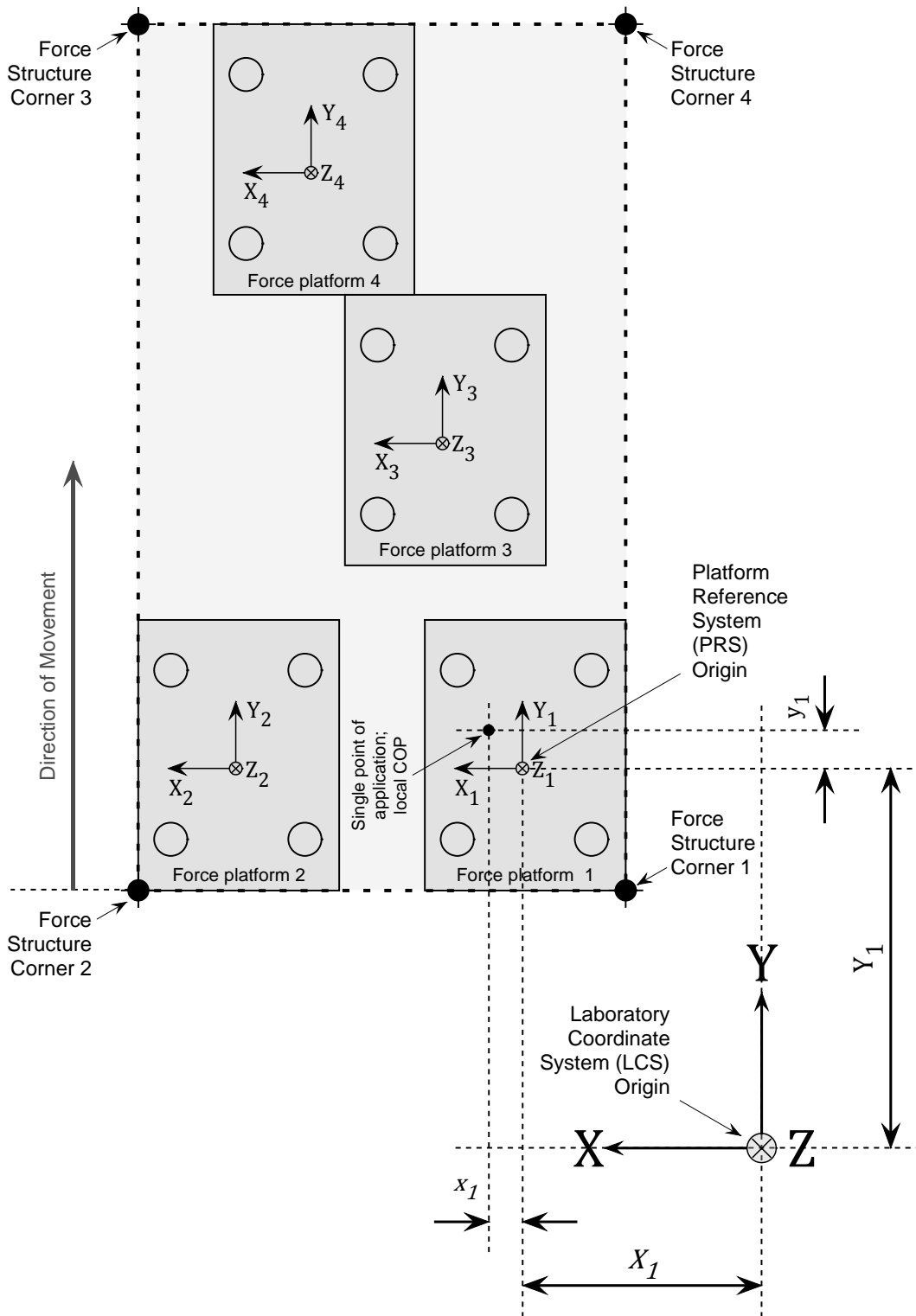
886
887 Figure 2.

888
889

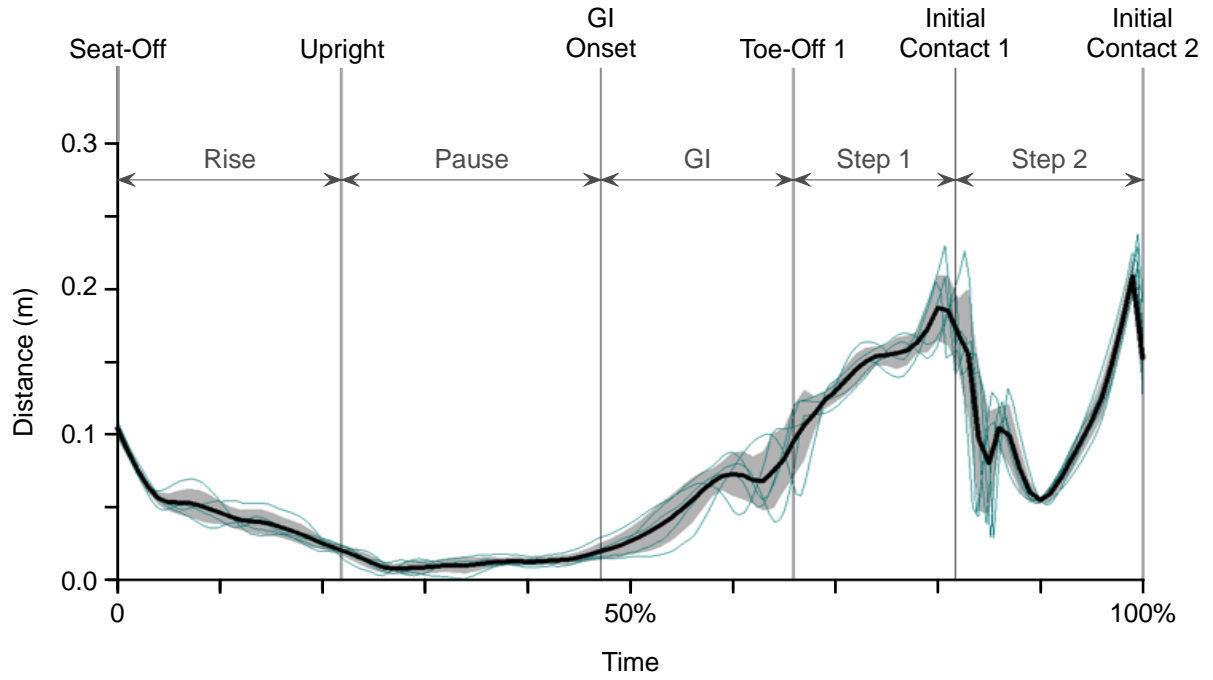


890
891 Figure 3.

892

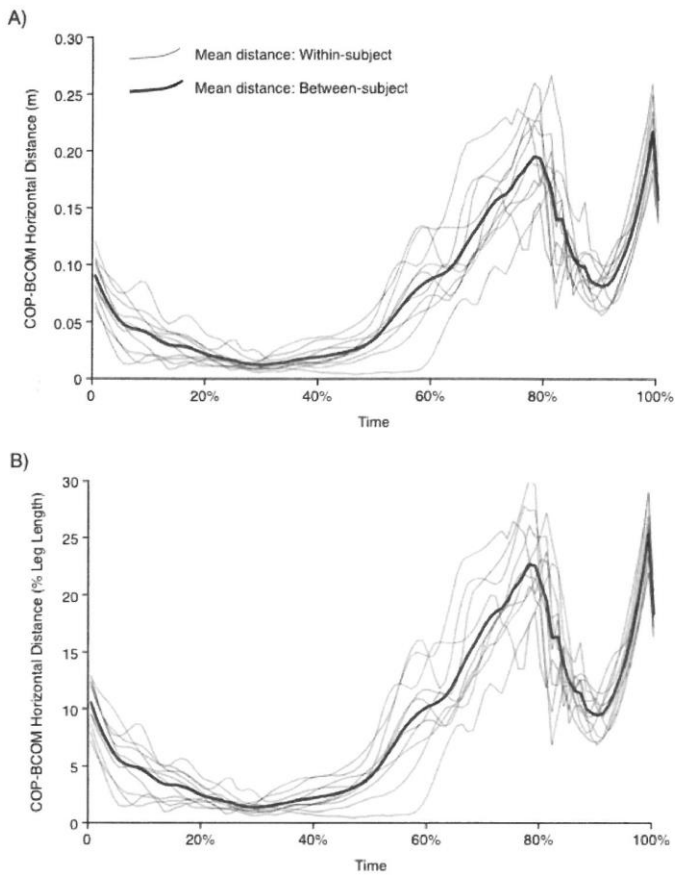


893
 894 Figure 4.
 895



896
897
898

Figure 5.



899
900
901
902

Figure 6.

Subject	Gender	Dominant Leg	Age (years)	KH (m)	120% KH (m)	Mass (kg)	Height (m)	Dom Leg Length (m)*
1	F	R	21	0.430	0.516	51.9	1.653	0.806
2	F	L	25	0.450	0.540	73.7	1.662	0.836
3	F	R	30	0.451	0.541	65.1	1.657	0.823
4	M	R	46	0.420	0.504	69.2	1.670	0.803
5	F	R	35	0.498	0.598	77.5	1.711	0.892
6	M	R	26	0.540	0.648	89.7	1.900	0.976
7	M	R	34	0.460	0.552	77.3	1.690	0.856
8	M	R	27	0.474	0.569	86.5	1.762	0.870
9	F	R	27	0.424	0.509	67.5	1.633	0.834
10	M	R	20	0.465	0.558	76.5	1.759	0.851
-	-	-	29.1 (±7.7)	0.461 (±0.036)	0.553 (±0.044)	73.49 (±10.87)	1.701 (±0.080)	0.885 (±0.051)

*Distance from hip joint centre to floor on dominant side

903
904
905

Table 1.

Segment	Label	No	Type [¶]	Descriptor
Head	TMJ	2	A	Temporomandibular joint
	VERT1	1	B	Vertex
	VERT2	1	T	Head tracking marker 2
	VERT3	1	T	Head tracking marker 3
Torso	JN	1	B	Most caudal aspect of jugular notch
	XP	1	B	Xiphoid process
	C7	1	B	Dorsal aspect of 7 th cervical vertebra spinous process
	T8	1	B	Dorsal aspect of 8 th thoracic vertebra spinous process
Pelvis	ASIS	2	B	Anterior superior iliac spine
	PSIS	2	B	Posterior superior iliac spine
Humerus	MHU	2	A	Medial humeral epicondyle
	LHU	2	B	Lateral humeral epicondyle
	AC	2	B	Acromioclavicular Joint
	HUM1	2	T	Humerus tracking marker 1
	HUM2	2	T	Humerus tracking marker 2
Forearm	HUM3	2	T	Humerus tracking marker 3
	RSY	2	A	Radial styloid process
	USY	2	B	Ulnar styloid process
	FRM1	2	T	Forearm tracking marker 1
	FRM2	2	T	Forearm tracking marker 2
Thigh	FRM3	2	T	Forearm tracking marker 3
	LEP	2	B	Lateral femoral epicondyle
	MEP	2	A	Medial femoral epicondyle
	THIGH1	2	T	Thigh tracking marker 1
	THIGH2	2	T	Thigh tracking marker 2
Shank	THIGH3	2	T	Thigh tracking marker 3
	THIGH4	2	T	Thigh tracking marker 4
	LML	2	B	Lateral malleolus
	MML	2	A	Medial malleolus
	TTB	2	A	Tibial tuberosity
	HFB	2	A	Fibula head

SHIN1	2	T	Shin tracking marker 1	
SHIN2	2	T	Shin tracking marker 2	
SHIN3	2	T	Shin tracking marker 3	
SHIN4	2	T	Shin tracking marker 4	
Foot	CAL	2	B	Upper ridge of the calcaneus posterior surface
	FM	2	B	First metatarsal
	VM	2	B	5 th metatarsal
	SM	2	A	2 nd metatarsal
Total: 71				
§Total: 63				

[¶]A – anatomical, T – tracking, B – both

[§]Total no. of markers for dynamic trials (No. of tracking markers)

906 Table 2.
907

Segment	Origin	Axes		
		x	y	z
Foot	Upper ridge of calcaneus (CAL)	Coincides with intersection between plane defined by CAL, 1st and 5th metatarsals (FM and VM), and its perpendicular plane containing CAL and 2nd metatarsal (SM), pointing forward	Mutually perpendicular to both x- and z- axis pointing upwards	Perpendicular to x-axis in plane defined by CAL, FM and VM pointing right
Shank	Midpoint between lateral and medial malleolus (LMAL and MMAL)	Mutually perpendicular to both y- and z- axis pointing forward	Coincides with intersection between plane defined by fibula head (HFB), LMAL and MMAL, and its perpendicular plane containing tibial tuberosity (TTB) and midpoint between LMAL and MMAL,	Perpendicular to y-axis in plane defined by HFB, LMAL and MMAL pointing right
Thigh	Midpoint between lateral and medial epicondyles (LEP and MEP)	Mutually perpendicular to both y- and z- axis pointing forward	Oriented from midpoint between LEP and MEP to hip joint center (HJC) pointing upwards	Perpendicular to y-axis in plane defined by LEP, MEP and HJC pointing right
Pelvis	Midpoint between right and left anterior superior iliac spine (RASIS and LASIS)	Perpendicular to z-axis in plane defined by RASIS, LASIS and midpoint between right and left posterior superior iliac spine (RPSIS and LPSIS)	Mutually perpendicular to both x- and z- axis pointing upwards	Oriented from LASIS to RASIS pointing right
Torso	Jugular notch (JN)	Perpendicular to y-axis in plane defined by C7, JN and midpoint between T8 and XP	Oriented from midpoint between JN and C7, and midpoint between T8 and xiphoid process (XP), pointing upwards	Mutually perpendicular to both x- and y- axis pointing right
Humerus	Shoulder joint center (SJC)	Mutually perpendicular to both y- and z- axis pointing forward	Oriented from midpoint between medial and lateral humeral epicondyles (MHU and LHU) to SJC pointing upwards	Perpendicular to y-axis in plane defined by MHU, LHU and SJC pointing right
Forearm	Midpoint between radial styloid (RSTY) and ulnar styloid (USTY)	Mutually perpendicular to both y- and z- axis pointing forward	Oriented from midpoint between RSTY and USTY to elbow joint center (EJC) pointing upwards	Perpendicular to y-axis in plane defined by RSTY, USTY and EJC pointing right
Head	Midpoint between right and left temporomandibular joints (RTMJ and LTMJ)	Mutually perpendicular to both y- and z- axis pointing forward	Oriented from origin to vertex (VERT1) pointing upwards	Perpendicular to y-axis in plane defined by RTMJ, LTMJ and VERT1 pointing right

909 Table 3a

910

Joint	Joint Center Definition
Glenohumeral	30 mm inferior to AC markers
Elbow	Mid point between MHU and LHU markers
Right Hip	x : 0.36*Distance between left and right ASIS
	y : 0.19*Distance between left and right ASIS z : 0.3*Distance between left and right ASIS
Left Hip	x : 0.36*Distance between left and right ASIS
	y : 0.19*Distance between left and right ASIS z : 0.3*Distance between left and right ASIS
Knee	Mid point between MEP and LEP markers
Ankle	Mid point between MMAL and LMAL markers

911

912 Table 3b

913

914

915

Event	Definition
Light-On	Instance determined as the point at which the light analogue channel voltage dropped below the mean-3SDs voltage for >8 frames (133ms) of 1 sec quiet sitting
Movement Onset	Instance determined when BCOM forward velocity increased for >8 frames (133ms) beyond the mean +3SD BCOM vertical velocity during 1sec of quiet sitting displacement before light-on
Peak Horizontal BCOM Velocity	Instance of peak horizontal (y-component) BCOM velocity signal occurring before seat-off event
Seat-Off	Instance determined as the point at which the seat-mat analogue channel voltage dropped below the mean-3SDs voltage for >8 frames (133msec) of 1 sec quiet sitting
Peak net Vertical GRF	Instance of peak summated force plates 1 and 2 vertical (z-component) GRF signal occurring between movement onset and seat-off events
Peak Vertical BCOM Velocity	Instance of peak vertical (z-component) BCOM velocity signal occurring between seat-off and upright events
Upright	Instance of initial peak vertical (z-component) BCOM displacement signal occurring between seat-off and first toe-off events
GI Onset	Instance when COP lateral velocity signal breaches 0.0m/s threshold for > 8 frames (133ms) occurring between Upright and HO1 events
Release	Instance when COP lateral velocity signal breaches 0.0m/s threshold for > 8 frames (133ms) occurring between GI Onset and HO1 events
1 st Toe-Off	Instance of swing limb force plate vertical (z-component) GRF signal <20N for >8 frames (133ms) occurring after Seat Off event
1 st Initial Contact	Instance of force plate 3 vertical (z-component) GRF signal >20N for >8 frames (133ms) occurring after TO1 event
2 nd Initial Contact	Instance of force plate 4 vertical (z-component) GRF signal >20N for >8 frames (133ms) occurring after IC1 event

916 Table 4.

917

918

Event	ICC (95% CI)*	S _w Distance [§] (m)	Repeatability Distance [†] (m)
Seat-Off	0.960 (0.900-0.989)	0.009	0.024
TO1	0.977 (0.943-0.993)	0.012	0.034
Step 1	0.976 (0.940-0.993)	0.012	0.032
Step 2	0.953 (0.884-0.987)	0.012	0.034

*Intra Class Correlation Coefficient for consistency, average variation, 2 way mixed effects, (95% confidence interval)

[§]Measurement error, mean intra-subject SD (S_w); the square root of the mean intra-subject variance

[†]An estimate of the maximum difference (m) between 2 observations with 95% confidence (2.77 S_w)

919 Table 5.

920
921

Subject	COP-BCOM Distance (m)				Maximum COP-BCOM Distance (m)			
	Seat-Off		TO1		Step 1		Step 2	
	Distance	Normalised*	Distance	Normalised	Distance	Normalised	Distance	Normalised
1	0.104 ±0.005	0.130 ±0.006	0.103 ±0.012	0.127 ±0.015	0.213 ±0.015	0.264 ±0.018	0.225 ±0.009	0.278 ±0.012
2	0.067 ±0.004	0.080 ±0.005	0.119 ±0.012	0.143 ±0.014	0.233 ±0.010	0.278 ±0.012	0.212 ±0.014	0.227 ±0.016
3	0.106 ±0.005	0.129 ±0.006	0.145 ±0.012	0.176 ±0.015	0.255 ±0.012	0.310 ±0.015	0.227 ±0.016	0.262 ±0.012
4	0.100 ±0.007	0.125 ±0.009	0.095 ±0.005	0.118 ±0.006	0.214 ±0.007	0.267 ±0.009	0.198 ±0.007	0.254 ±0.012
5	0.078 ±0.006	0.087 ±0.006	0.180 ±0.011	0.201 ±0.013	0.278 ±0.018	0.312 ±0.020	0.262 ±0.012	0.256 ±0.014
6	0.120 ±0.007	0.123 ±0.007	0.194 ±0.015	0.199 ±0.015	0.304 ±0.016	0.311 ±0.016	0.254 ±0.012	0.280 ±0.011
7	0.103 ±0.006	0.120 ±0.007	0.148 ±0.015	0.173 ±0.018	0.289 ±0.007	0.337 ±0.008	0.256 ±0.014	0.245 ±0.010
8	0.062 ±0.007	0.072 ±0.008	0.129 ±0.012	0.149 ±0.013	0.244 ±0.010	0.280 ±0.011	0.249 ±0.008	0.190 ±0.011
9	0.080 ±0.006	0.096 ±0.007	0.099 ±0.012	0.118 ±0.015	0.204 ±0.008	0.245 ±0.010	0.190 ±0.011	0.228 ±0.015
10	0.081 ±0.021	0.095 ±0.025	0.143 ±0.014	0.169 ±0.016	0.257 ±0.008	0.302 ±0.009	0.228 ±0.015	0.230 ±0.025
All	0.090 ±0.019	0.106 ±0.022	0.135 ±0.033	0.157 ±0.031	0.249 ±0.034	0.291 ±0.028	0.230 ±0.025	0.230 ±0.025
COV†	21.2%	20.8%	24.7%	19.7%	13.6%	9.7%	10.8%	10.8%

*Normalised COP-BCOM distance as a proportion of dominant toe
†Coefficient of variation (SD/mean as a percentage) between

922
923 Table 6.